

# Rules For Deriving Basic Semiconductor Region Models

Bruno ALLARD, member IEEE, Hervé MOREL, Chung-Chieh LIN, Hichem HELALI, Jean-Pierre CHANTE, member IEEE

CENTRE DE GENIE ELECTRIQUE DE LYON

(CEGELY - URA CNRS 829)

INSA/ECPA, Building 401,

20, avenue Albert Einstein

F-69621 Villeurbanne Cedex. France

Fax : (+33) 72438530 / Email : allard@cegely.insa-lyon.fr

**Abstract** - We discuss some main rules for deriving power semiconductor device modular models. The method is based on the classical regional hypothesis that parts any power semiconductor device in basic semiconductor regions as : the neutral ohmic region, the gradient-doping neutral region, the high-level injection region, the space-charge region and the field-effect region. But specific rules have to be observed in the model definition in order to obtain reusable models. Then a power semiconductor device model becomes a simple association of several of the basic semiconductor region models : a bond graph. The space charge region model description is covered. Significant results are presented.

## I - INTRODUCTION

CAD is hardly used in power electronic field today. One main reason is that power semiconductor device accurate models are not available except the power MOS transistor model. In fact numerous works concerned the power MOS transistor while few works focused on the bipolar power semiconductor devices. We may note that the published results are not fully satisfying! For example the commercially available simulators Saber and Spice do not offer any PIN diode model or any power bipolar transistor model.

The main difficulty is the occurrence of a high-level injection region inside the bipolar power semiconductor devices. This layer reduces the on-state device voltage drop but also increases the turn-off transient. The high-level injection region (HIR) is the area of carrier storage that is a distributed phenomenon, described by the ambipolar diffusion equation (partial differential equation).

We have already proposed power bipolar semiconductor device models [1-5]. Particularly we have shown [2,3] that the Internal Approximation method (a Variational Approximation technique) enables to derive a HIR state-variable model, a set of ordinary and differential equations (depending on the time variable). The method most important advantage is to yield a low-cost state-variable model compared to the discretization techniques [6]. The HIR model brings a real improvement to the PIN diode model compared to other available models [7].

We have successfully applied the method to the power bipolar transistor model [4].

We thought then to reuse the same HIR model in the power BJT and PIN diode models as the physical phenomena are the same.

In fact the one-dimension HIR (figure 1) is governed by the ambipolar diffusion equation (1) with the boundary conditions (2) and (3).

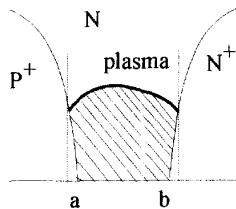


figure 1 : a typical high-level injection region.

$$(1) \quad \frac{\partial p}{\partial t} = D \cdot \frac{\partial^2 p}{\partial x^2} - \frac{p}{\tau}$$

$$(2a) \quad p(t, a) = |\Gamma(a)|$$

$$(2b) \quad p(t, b) = |\Gamma(b)|$$

$$(3a) \quad qDA \frac{\partial p}{\partial x}(t, a) = i_p(t, a) - \frac{\mu_p}{\mu_n + \mu_p} \cdot i(t)$$

$$(3b) \quad qDA \frac{\partial p}{\partial x}(t, b) = i_p(t, b) - \frac{\mu_p}{\mu_n + \mu_p} \cdot i(t)$$

where  $t$  is the time variable, and  $x$  the geometrical variable,  
 $p(t, x)$  is the hole concentration (minority carriers),  
 $a(t), b(t)$  are the HIR boundary abscissa,  
 $\Gamma(x)$  is the net doping concentration,  
 $\mu_n$  and  $\mu_p$  are the carrier mobility,  
 $D$  is the ambipolar diffusion coefficient,  
 $A$  is the HIR active area,  
 $i(t)$  is the total current crossing the HIR,  
 $i_p(t, a), i_p(t, b)$  are the minority carrier (hole) currents at the HIR boundaries.

The equation set (1) to (3) is the same for the PIN diode and the bipolar transistor. The only differences are to be found in the variable values introduced in the boundary equations :  $p(a), p(b), a, b, i_p(a), i_p(b)$  and  $i$ . Thus if we build a HIR model where the external environment is represented by the latter variables, we will obtain a reusable HIR model for the case of the PIN diode and the bipolar transistor.

We just have seen how the HIR model external variable choice is important if the model is to be reusable.

This paper deals with the main rules to be applied in order to obtain modular and reusable basic semiconductor region models (section 2). The section 3 covers the space charge region model description using the Pacte software M++ language. Pertinent results are presented in the section IV.

## II - THE MODULAR MODELLING BASIC RULES

### THE BASIC SEMICONDUCTOR REGIONS

We have seen that a HIR is present both in the PIN diode, in the power bipolar transistor and generally in all bipolar power devices.

The HIR has been enlighten applying the regional hypothesis that is a classical hypothesis in semiconductor device modelling.

In fact the semiconductor equations - the Poisson equation, the hole and electron transport equations - do not have the same importance in the different regions of a semiconductor device. One lonely main physical phenomenon may often be observed in any given region of the device.

Then we may list easily the usual basic semiconductor regions (BSRs) where only one physical phenomenon is acting [9] (table 1).

<i>basic semiconductor region</i>	<b>Poisson equation</b>	<b>condition for the majority carriers</b>	<b>condition for the minority carriers</b>	<b>majority carrier transport</b>	<b>minority carrier transport</b>
<i>space charge region</i>	principal	quasi constant current	quasi constant current	drift	drift
<i>neutral ohmic region</i>	negligible	concentration equal to doping	recombination	drift	diffusion
<i>non uniform doping neutral region</i>	negligible	concentration equal to doping	recombination	drift-diffusion balance	drift and diffusion
<i>high-level injection region</i>	negligible	equal majority and minority carriers concentration. ambipolar diffusion	equal majority and minority carriers concentration. ambipolar diffusion	drift and diffusion	drift and diffusion

table 1 : the main types of behaviour inside the bipolar power semiconductor devices

In order to avoid sign error in the BSR model equations, we may notice that it is advised to consider minority and majority carriers instead of holes and electrons.

#### THE EXTERNAL VARIABLES.

Once all the BSRs have been defined, the model external variables have to be specified as we have seen before for the HIR. But we want that the association of the BSR models keeps as simple as a game. So we must limit the number of the external variables. Moreover it is suitable to choose one list for all the BSR models.

As a guide for the latter choice, we have examined the main methods of model association, that is to say the methods yielding the equation set of a given system.

Three main methods are to be considered. The most classical is the nodal method (*Kirchhoff network*) that describes the connections between all the components of a network. This method is used in Spice and Saber. An other important method is the *block diagram description*. It explicitly defines the direction of the information flows what does not perform the nodal method.

The block diagram description is used in Automatics and Mechanics. Numerous softwares accept this system description input format : Tutsim, Matlab, Acsel ...

The bond graph techniques is described in [10]. But as this method is not usual in electronics, we think important to recall same main points [11].

Born 30 years ago, this method wants to take the advantages of the two former methods and to unify the description of the dynamic behaviour of any physical system. It is a network-like method but it is also a causal method as it comprises the system causality analysis that states out the direction of the information flows. The bond graph technique underlying idea is to represent a physical system from the energy viewpoint. The power characterising the energy is expressed as the product of a *flow-variable* and an *effort variable*.

In the case of the semiconductor device, the energy flows are linked to the free carrier transports. The potential energy flow is the electric energy (current, voltage). The carrier kinetic energy is mostly the hydraulic energy flow (volume flow, pressure), with the ideal gaz hydrodynamic hypothesis.

The table 2 lists the flow variable and the effort variable which product characterises the power associated to the two former energy flows.

Finally we think that the bond graph technique [10] is the most efficient method in the case of our modelling problem.

#### MOVING BOUNDARIES

It appears as an evidence that care must be taken in the model derivation because of the semiconductor region moving boundaries.

#### THE BASIC SEMICONDUCTOR REGION MODEL PARAMETERS

Consequently the BSR model parameters should be the parameters representing the main physical phenomenon in the BSR. The table 3

lists the region main parameters.

It may be noted that there are very few parameters compared to the electrical parameters of the classical equivalent circuit models. But their identification is not simple.

The technological parameter identification is out of the scope of this paper but details may be found in [13].

<i>energy flow</i>	<b>flow variable</b>	<b>effort variable</b>
<i>electric</i>	current, $i$	voltage, $u$
<i>hydraulic (related to electrons)</i>	volume flow $f_n = A \cdot v_n$	pressure, $P_n = n \cdot kT$ ( $n$ is the electron concentration)
<i>hydraulic (related to holes)</i>	volume flow $f_p = A \cdot v_p$	pressure, $P_p = p \cdot kT$ ( $p$ is the hole concentration)
<i>heat</i>	entropy flow $f_s$	temperature $T$

table 2 : the main energy flows across a semiconductor region cross-area  $A$ . The carrier gas are considered as ideal.  $k$  is the Boltzmann constant.

#### THE STATE-VARIABLE MODELLING

The state-variable modelling technique [12] is a general physical system modelling frame. A state-variable model is an Algebraic and Ordinary Differential Equation set. We may add that the bond graph analysis of a physical system leads to a state-variable representation of the different components of the system. In fact a state-variable model takes care of the memory effect inside a system basic component. This memory effect is always associated to an energy storage.

So a physical system bond graph should represent the energy flows between the system basic components while the basic component state-variable model should describe the energy storage inside the component.

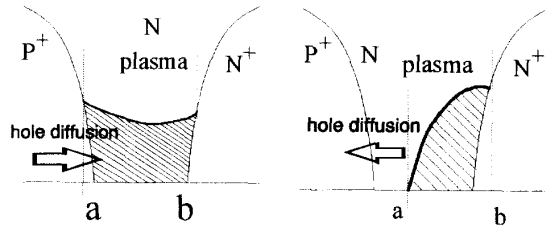


figure 2 : a typical HIR in the saturation state.

figure 3 : a typical HIR in the recovery state.

#### THE CHANGE IN THE MODEL CAUSALITY

We take the example of the minority carrier current  $i_m(t,a)$  at one boundary of the HIR in order to illustrate the change in the HIR model causality. (Note that the holes are now considered as the minority carriers, in order to ensure the model use in the case of a N-doped or a P-doped HIR). The question is to point out which BSR is in charge of the minority carrier current  $i_m(t,a)$  value computation.

When the HIR exists and is in the saturation case (figure 2), the minority carrier current  $i_m(t,a)$  is easily derived from the total current and the current associated to the minority carrier recombination in the P+ lateral layer. The minority carriers (the electrons) diffused across

basic semiconductor region	silicon material general parameters	length, W	doping profile, $\Gamma$	doping profile gradient $\Gamma'$	active area, A	ambipolar lifetime, $\tau$	minority carrier lifetime, $\tau_m$
space charge region	X	-	X	X	X	-	-
neutral ohmic region	X	X	X	-	X	-	X
non uniform doping neutral region	X	X	X	X	X	-	X
high-level injection region	X	X	-	-	X	X	-

table 3 : the basic semiconductor region models main parameters

the space-charge region from the HIR to the lateral P+ region. During a recovery transient the space-charge region prohibits this latter transport of electrons and the current  $i_m(t,a)$  cannot anymore be derived from the lateral P+ layer recombination current. On the other hand this current  $i_m(t,a)$  corresponds to the diffusion of holes from the HIR to the lateral P+ layer. Then the value of  $i_m(t,a)$  is yielded by the equation (3a).

This phenomenon is a causality change : the semiconductor region that yields the current  $i_m(t,a)$  changes depending on the operation mode (saturation/recovery).

In the case of a non-causal method (nodal method for example), we are lead to solve this problem by writing two implicit equations. These are two constraint equations that lead to a ill-conditioned equation system (stiff problem).

We have already proposed a method to take advantage of the causality change [11]. This method also applies in the case of a change in the behaviour of a BSR.

#### THE CHANGE IN THE PHYSICAL BEHAVIOUR

The change in the physical behaviour is a classical problem in power electronics. The notions of on-state and off-state are classical when dealing with a switch.

We now take the example of the space charge region that shows a drastic change in its behaviour.

In the classical depletion state (figure 4) the space charge region shows a capacitive behaviour. There is an equivalent storage of electrostatic charges of opposite sign. The Poisson equation then yields the relation between this storage charge and the total voltage drop at the boundaries of the region. A simple charge balance gives the state-equation of this BSR model.

When a HIR exists at one boundary of the space charge region (figure 5), the region is drastically narrowed and its behaviour becomes complex to describe. There is a large interaction between the Poisson equation and the transport equations. But the space charge region has a very small influence on the power device general behaviour. Then this space charge region can be neglected with a good approximation. The basic region model is then reduced to the continuity of the external variables between the two lateral regions.

The next section explains how it can be taken a large advantage of the changes in the BSR behaviour or in their model causality.

#### THE DYNAMIC MODEL SWITCHING

As there are changes both in the BSR behaviours and in their model causality, an idea is to write as many state-variable models as there are changes. Concerning a given BSR there will be as many models as the region shows different behaviours.

Then the idea is to change the region model dynamically during the simulation according to the system global state. The time-moment when the model switching appears, depends on the validation of transitions between the different models.

We have proposed the Petri net technique [9, 11] to manage the dynamic model switching. Broadly speaking this technique replaces all the conditional "if .. then .. else" structure of classical representation by state transitions.

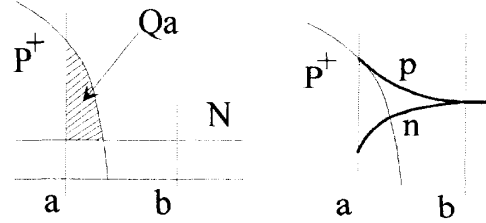


figure 4 : a typical space charge region in the depletion state.

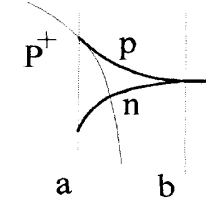


figure 5 : a typical space charge region narrowed because of a high-level injection region at one boundary.

A bond graph describes the system dynamic behaviour while a Petri net describes the system functional behaviour.

We have already shown [11] that the two coupled techniques enable to spare a high amount of simulation CPU time. The table 4 sums up the result of same comparisons between Saber v3.2 and Pacte v0.9.1. [14].

The next section covers the space charge region model description using the Pacte M++ language. We may say immediately that the translation between the Pacte M++ language and the Saber Mast language is easy when dealing with a one-state model. Of course the translation is not possible in the case of multi-states model as Saber does not support the dynamic model switching process.

It is worth noting that Pacte enables to cut down the simulation time only thanks to the original methods used at the modelling and simulation levels compared to Saber that is a full mature product from computer-science viewpoint.

test circuit	SABER 3.2	PACTE 0.9.1	ratio SABER/PACTE
ideal chopper	76.7s	14.91s	5.14
PIN4	18.4s	4.65s	3.96
chopper/ PIN4	230.0s	84.3s	2.73
chopper/ PIN9	-	35.1s	7.61

table 4 : simulation time comparisons between Saber and Pacte on a SparcStation II. The ideal "chopper circuit" includes ideal switches and a classical closed-loop. The circuit "PIN4" tests the recovery process of a power diode using the Pacte state-variable model PIN4 that has been also translated for Saber. The circuit "chopper/PIN4" includes a classical power MOS model and the power diode PIN4 model. The circuit "chopper/PIN9" includes the power diode PIN9 model that invokes the dynamic model switching process.

### III - THE SPACE CHARGE REGION MODEL DESCRIPTION

The space charge region model has only one state-variable. It is thus much less complex than the HIR model (described in [3]). It has been chosen as a tutorial example. Whatever, all the BSR models are available upon request to the authors.

The figure 6b pictures the bond graph symbol of the space charge region model and its related Petri net.

The symbol has 8 bonds (half-arrow). These bonds transfer different types of energy : hydraulic energy related to the majority carriers ( $MD$ ,  $Me$ ) and to the minority carriers ( $mD$ ,  $me$ ), and the electrical energy

( $xL$ ,  $xe$ ). The bonds  $aD$  and  $ae$  do not transfer energy, they are geometrical bond that carry the information "region geometrical boundaries".

As described there-above the space charge region presents a change in its behaviour that leads to a Petri net with three places describing : the depletion state, the non-existing state and a static state that eases the global system simulation initial point computation.

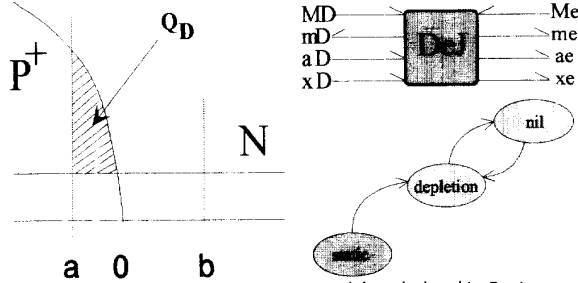


figure 6 : the space charge region model symbol and its Petri net

In the space charge region (figure 6a) the depletion hypothesis enables to separate the Poisson equation and the transport equations. The depletion layer extends from the abscissa  $a$  in the diffused P+ layer to the abscissa  $b$  in the low-doped epitaxial layer. The doping profile is approximated by (4). The electric field value at the left boundary yields one boundary condition (5).

$$(4) \quad \Gamma(x) = \chi_D \cdot N \cdot \left[ 1 - \exp\left(-\frac{x}{r_D}\right) \right]$$

$$(5) \quad E_D = \chi_D \cdot u_T \cdot \left. \frac{d \ln |\Gamma(x)|}{dx} \right|_{(x=a)}$$

where  $\chi_D$  is equal to +1 in the case of a P+N junction and -1 in the case of a N+P junction,  
 $r_D$  defines the doping gradient in the diffused layer near the junction,  
 $u_T = k \cdot T / q$  is the thermal voltage,  
 $N$  is the epitaxial layer uniform doping concentration.

The problem is then normalised with respect to the value  $x_D$ . The abscissas become  $\alpha$  and  $\beta$ , the geometrical variable becomes  $y$  and the electric field becomes  $e(y)$ . The normalised doping profile is  $\gamma(y)$  and we define the undimensional value  $r$ .

The Poisson equation yields (6) :

$$(6) \quad \frac{de}{dy} = \frac{\chi_D}{r} \cdot \gamma(y), \quad \text{with} \quad r = \frac{\epsilon \cdot u_T}{q \cdot N \cdot r_D^2}$$

If the following primitive functions of  $\gamma(y)$  are noted  $H(y)$  and  $I(y)$ , then the Gauss Theorem gives (7) and the total barrier height is computed as (8).

$$(7) \quad r \cdot (e(\beta) - e(\alpha)) = \chi_D \cdot (H(\beta) - H(\alpha))$$

$$(8) \quad u_B = \gamma_c \cdot [I(\alpha) - I(\beta) + H(\alpha) \cdot (\beta - \alpha)] + \gamma_{xc} \cdot e(\alpha) \cdot (\beta - \alpha)$$

Finally the First Law of the Thermodynamics gives the model state equation. It is only a charge balance equation in one-half of the space charge region, for example between  $a$  and  $0$  (9).  $Q_D$  is the model state-variable.

$$(9) \quad \frac{dQ_D}{dt} = i_m(\beta) - i_m(\alpha)$$

$$\text{where} \quad Q_D = q \cdot A \cdot \int_a^0 \Gamma(x) \cdot dx = -\chi_D \cdot q \cdot N \cdot A \cdot x_D \cdot H(\alpha),$$

$i_m(\beta)$  and  $i_m(\alpha)$  are the minority carrier currents at the region boundaries.

The Pacte M++ language syntax is closed to the C++ syntax. Then it enables to describe the space charge region model as a class (see next page and Object Oriented Programming formalism).

The model description file begins by the declaration of the model *DeJ* (class) with the list of ports, the list of states, the constructor and the list of local variables. We draw the reader attention about the dimension analysis that prevents a lot of errors.

One important file is "physics.u" that collects all the physical dimensions with their ISO unit or usual units.

The port list describes the model bonds, then it readily defines the model external variable. Each port declaration includes the statement of an energy type, and the external variable (flow and effort) names.

The following section concerns the constructor with the list of parameters and the computation of the local variables. The different states are described one after one.

The declaration of a *state* includes the name of the state variables (only one in the present case). The equation of a state are sequential equations (using the sign =), causality equations (computation of the external variables : the voltage drop, the region abscissas, minority or majority carrier concentrations ...), and implicit or state-equations (using the sign ==). The condition that validates a transition to another *state* is written explicitly through a "if.." structure.

The figure 7 pictures the other BSR model symbols. All the symbols show the same 4 kinds of port (where are connected the bonds) : majority and minority carrier hydraulic energy bonds, electrical energy bonds and geometrical bonds.

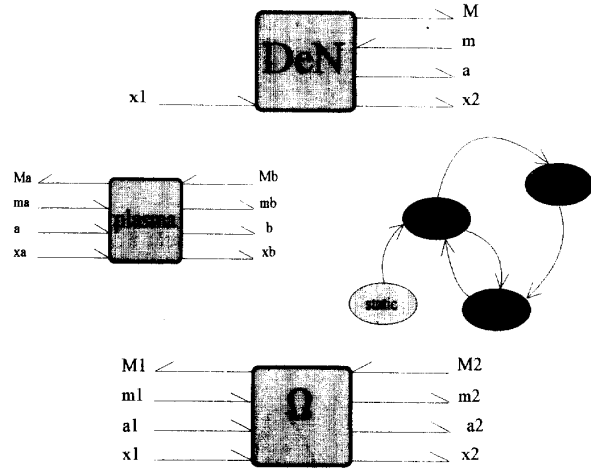


figure 7 : other BSR model symbols : DeN, neutral gradient-doping region; Plasma, HIR;  $\Omega$ , neutral ohmic region.

The HIR Petri net presents 4 states : the classical saturation and recovery states, the "non-existing" state when the high-level injection hypothesis is not met, and a static state used in a system initial point computation.

#### IV - SIMULATION RESULTS

##### THE MAIN POWER DEVICE MODEL DEFINITION

We have defined 4 main BSRs : the neutral ohmic region, the gradient-doping neutral region, the HIR and the space charge region. We have described and compiled the related models.

```

////////////////////////////////////
// CEGELY - Insa de Lyon
// basic semiconductor regions
//
// Diffusion Epitaxy Junction model
// (DeJ)
/*
KhiD is the sign of the diffusion region:
KhiD = 1 for P+n
KhiD = -1 for N+n
the doping profile is defined by
Gamma(x) = KhiD*Nj*(1-exp(-x/xD));
the junction is defined for x1 < x < x2
w = (x2-x1)/xD is the normalized
space charge region length
y1 = x1/xD;
y2 = x2/xD;
notice that y1 < 0 < y2;
*/

#include <physics.u>

model DeJ
{
  /// Diffusion side
  port hydraulic input MD(fMD,PMD);
  port hydraulic output mD(fmD,PmD);
  port geometric input aD(faD,aD);
  port electric input xD(i,vD);
  /// Epitaxy side
  port hydraulic output me(fme,Pme);
  port hydraulic input Me(fMe,PMe);
  port geometric output ae(fae,ae);
  port electric output xe(i,ve);
  /// list of states
  state depletion(none w);
  state nil();
  slow state static() {none w};
  /// constructor declaration
  DeJ(none khiD,
    area deviceArea,
    length dopingGradient,
    length junctionDepth,
    length baseWidth,
    length dopingGradient2,
    concentration Nj,
    temperature T);
  /// physical constants
  charge q = 1.602e-19 C;
  entropy k = 1.38e-23 J/K;
  /// silicon constants
  dielectricConstant eps = 1.045e-10 F/m;
  speed vs = 1.0e7 cm/s;
  concentration ni = 1.45e10 cm-3;
  /// local variable computation
  khiD = index;
  uT = k*T/q;
  uKhiD = khiD*uT;
  /// current convention
  /// uKhiD*iMD = PMD*fMD;
  /// uKhiD*iMD = PmD*fmD;

  concentration Nj;
  temperature T;
  /// list of local variables
  const voltage uT, uB0, uKhiD;
  const energyDensity Uj;
  const energy Ud;
  const length xD, xJ;
  const area A;
  const none r, khiD;
  const none w01, y1_02, y2_02;
  const carrierFlow fs;
  const charge QjD;
  const none ro0;
  const none yB,aB;
  const current ime0;
  none G1,G2,H1,H2,I1,I2;
  current ime,iMD;
  none uB;
  none gamma0;
  };

  /// constructor////////////////////////////////////
  DeJ::DeJ(none index,
    area deviceArea,
    length dopingGradient,
    length junctionDepth,
    length baseWidth,
    length dopingGradient2,
    concentration Nj,
    temperature T)
  {
    /// physical constants
    charge q = 1.602e-19 C;
    entropy k = 1.38e-23 J/K;
    /// silicon constants
    dielectricConstant eps = 1.045e-10 F/m;
    speed vs = 1.0e7 cm/s;
    concentration ni = 1.45e10 cm-3;
    /// local variable computation
    khiD = index;
    uT = k*T/q;
    uKhiD = khiD*uT;
    /// current convention
    /// uKhiD*iMD = PMD*fMD;
    /// uKhiD*iMD = PmD*fmD;

    // uKhiD*iMe = Pme*fMe;
    // uKhiD*iMe = Pme*fme;
    Uj = k*T*Nj;
    area Ld2 = eps*uT/q/Nj;
    xD = dopingGradient;
    xJ = junctionDepth;
    A = deviceArea;
    r = Ld2/xD/xD;
    none r24 = 24*r;
    none phiJ = ln(Nj/ni);
    none u00 = r24*(phiJ-ln(2));
    none w00 = pow(u00,1/3);
    w01 = pow(u00+r24*ln(w00),1/3);
    none w02 = 1+sqrt(1+4*phiJ*r);
    none ro02 = exp(-w02);
    none z1_02 = w02/(1-ro02);
    none z2_02 = ro02*z1_02;
    y1_02 = -ln(z1_02);
    y2_02 = -ln(z2_02);
    uB0 = khiD*uT/r;
    fs = A*vs;
    Ud = Uj*A*xD;
    QjD = khiD*q*A*Nj*xD;
    ro0 = 1.5;
    yB = baseWidth/xD;
    aB = dopingGradient/
      dopingGradient2;
    ime0 = khiD*q*Nj*A*vs;
  }

  //////////////////////////////////////
  state DeJ::depletion(none w)
  {
    none ro = exp(-w);
    none z1 = w/(1-ro);
    uB = (z1*w-w*(1+w/2))/r;
    /// voltage drop
    (ve = vD+uB*khiD*uT |
     vD = ve-uB*khiD*uT);
    /// transition to state nil
    if (uB < 1) nil();

    none y1 = -ln(z1);
    none y2 = w+y1;
    aD = xD*y1;

    ae = xD*y2;
    /// pn is constant in the SC region
    PmD = Pme *exp(-uB);
    Pme = PMD*exp(-uB);
    ime = Pme*fme/uKhiD;
    current imD = PmD*fmD/uKhiD;
    iMD = i-imD;
    fMD = (iMD*uKhiD)/PMD;
    current iMe = i-ime;
    fMe = (iMe*uKhiD)/PMe;

    /// state equation
    dH1/dt = (ime-iMD)/QjD;
    /// where H1=H(y1)=y1+z1-1
    /// =z1-ln(z1)-1;
    none dH1_dz1 = 1-1/z1;
    none dz1_dw = (1-ro*z1)/(1-ro);
    w' = (ime-iMD)/QjD/dH1_dz1/dz1_dw;
  }

  //////////////////////////////////////
  state DeJ::nil()
  {
    length w = 2.5um;
    aD = ae -w;
    fae = 0 J/s/m;
    uB = 1;
    (ve = vD+uB*khiD*uT |
     vD = ve-uB*khiD*uT);

    Pme = PMD/ro0;
    PmD = Pme/ro0;
    fMe = fmD/ro0;
    fMD = (i*uKhiD - PmD*fmD)/PMD;

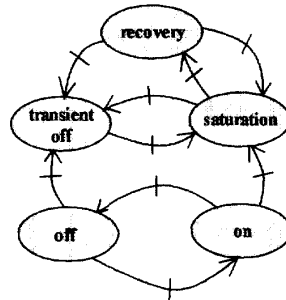
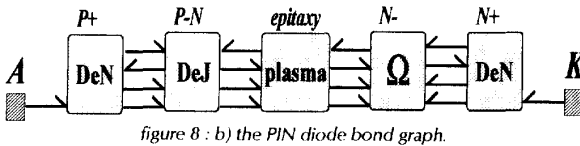
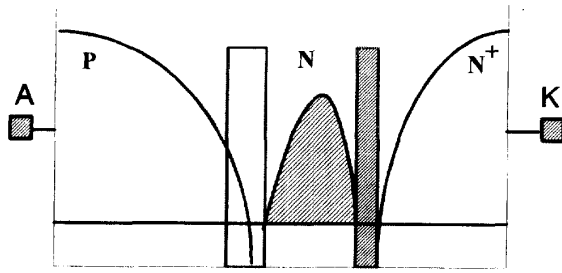
    if (depletion) depletion(1.2);

    ime = Pme*fme/uKhiD;
    iMD = PMD*fmD/uKhiD;
  }

```

The space charge region model declaration file using the Pacte M++ language.

Now the model of any power device is obtained easily by association of the BSR models according to the technological structure of the device.



For example the figure 8a shows the typical technological structure of the PIN diode and the figure 8b pictures the derived bond graph (the PIN diode model). We may note that each cross-section between two BSRs is represented by 4 bonds : one electrical bond, 2 hydraulic bonds and one geometrical bond. The reader may refer to the figure 7 to see how these bonds are declared in the BSR model. An automatic method [11] yields the PIN diode model related Petri net taking into account the Petri net of the different BSR models that compose the device (figure 8c).

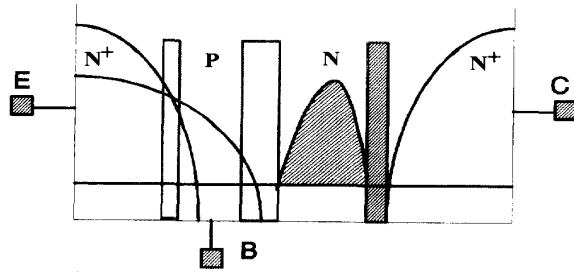


figure 9 : a) the power bipolar transistor typical structure

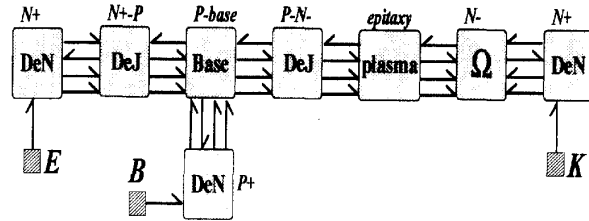


figure 9 : b) the power bipolar transistor bond graph.

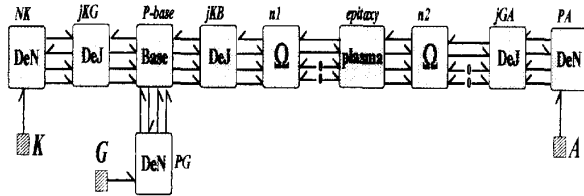


figure 10 : the GTO bond graph.

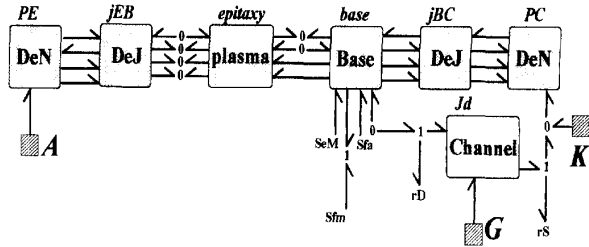


figure 11 : the IGBT bond graph.

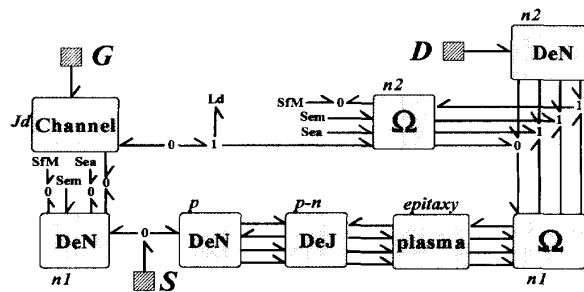


figure 12 : a) the power MOS transistor bond graph.

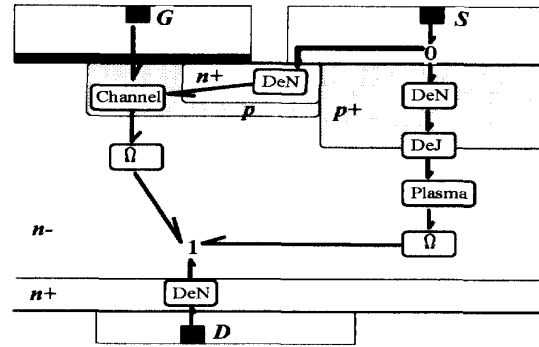


figure 12 : b) the power MOS transistor bond graph superimposed to the device technological structure.

It is easy to build the model of the power bipolar transistor (figure 9), the GTO (figure 10), the IGBT (figure 11) or the power MOS transistor (figure 12a).

The reader may note for example that the power MOS transistor model includes naturally the internal body diode that is sometimes used in power converters (figure 12b).

#### SIMULATION RESULTS.

We have obtained satisfying simulation results in the case of the five former power devices, using only the same 6 BSR models. We now present some significant results.

We have used the model in figure 8 to simulate a PIN diode typical turn-off transient. The figure 13 shows the simulation results and the experimental results.

The simulation starts when the PIN diode is in the state "saturation" (see figure 8c).

At  $t=37\text{ns}$ , a significant space charge region appears and validates a transition to the state "recovery" of the PIN diode model. At  $t=90\text{ns}$ , the high-level injection hypothesis stops to be valid and the PIN diode model enters the state "transientOff".

The evolution of the high-level injection region boundaries are plotted in the bottom of figure 13. The HIR model gives also an accurate approximation of the minority carrier concentration evolution as shown in figure 14. These information are not readily useful for a circuit design engineer, but enable a practical evaluation of the HIR model in comparison with device simulators.

The figure 15 pictures a switching cycle of a GTO under an inductive load.

The figure 16 pictures a switching cycle of a power MOS transistor under inductive load ( $22\mu\text{s} < t < 32\mu\text{s}$ ). The device starts in the reverse conduction state in order to stimulate the body diode ( $9\mu\text{s} < t < 10\mu\text{s}$ , body diode turn-off).

The figure 17 pictures a turn-off transient of the IGBT. The simulation conditions are the same as those applied in [15] where the Hefner IGBT model is used.

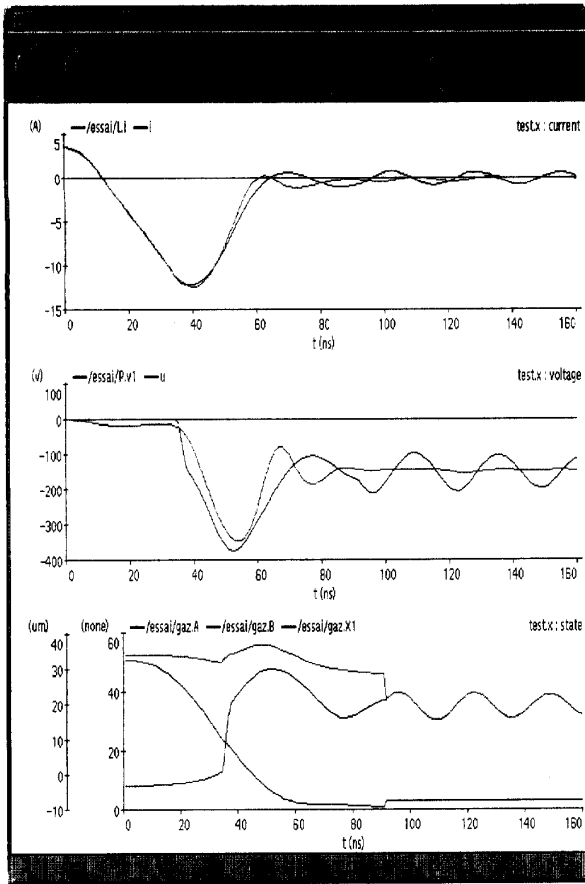


figure 13 : A typical PIN diode turn-off transient. Top) experimental and simulation current waveforms. Middle) experimental and simulation voltage waveforms. Bottom) the HIR boundary abscissas (A, B) evolution and the total charge storage (X1) evolution.

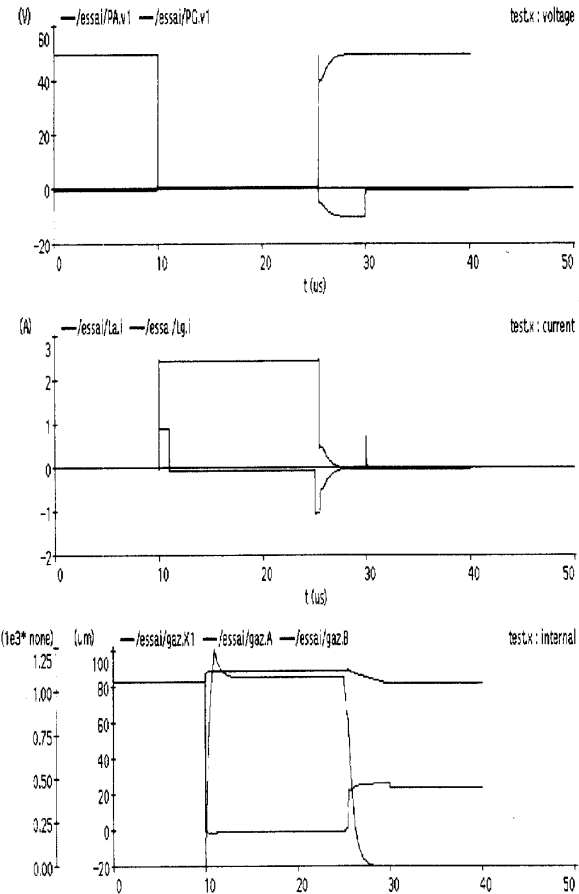


figure 15 : typical CTO voltages  $v_{AK}$  and  $v_{GK}$ , currents  $i_A$  and  $i_C$ , HIR boundary abscissas (A, B) and total storage charge (X1) during turn-off.

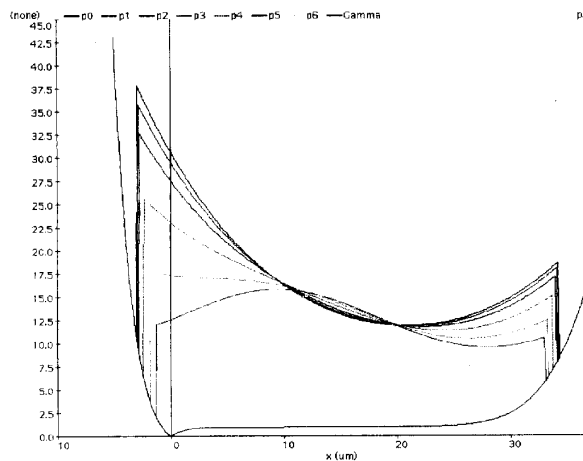


figure 14 : evolution of the minority carrier doping profile in the HIR during the turn-off transient and before the space-charge region appears again.

## V - CONCLUSION

The power device modelling is not something easy. Nevertheless some rules and original methods enables to write modular and efficient models. The bond graphs of the main bipolar power devices are obtained easily by association of only 6 reusable BSR models. The modularity aspect eases the overall improvement of the models. We have implemented the dynamic model switching technique. It simplifies the model description in the case of changes in the behaviour or in the model causality. The dynamic model switching cuts down the simulation cost. It has also enabled to derive 5 power device models using only 6 same BSR models. Thanks to this technique, the development of a new device model is easy. We hope to develop as many particular models as needed. On the other hand the BSR models may look complex. But the primary simulation comparisons (with Saber) show comparable or better simulation CPU time than with classical Spice models, and with a real accuracy concerning the power semiconductor devices.

A complete tool (editor, compiler, debugger) is available to implement the models using a high-level language (M++, Pacte).

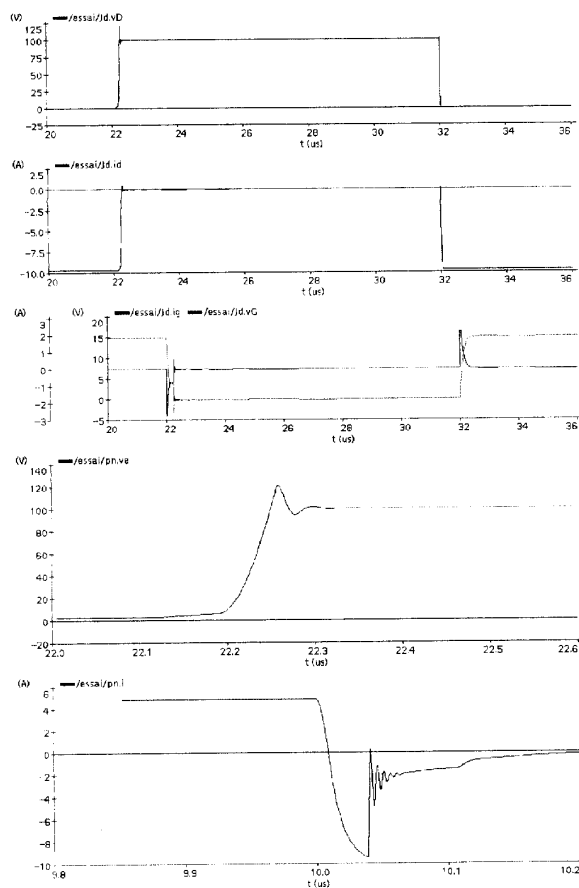


figure 16 : typical MOS voltage  $v_{DS}$  and currents  $i_D$  and  $i_G$  during a turn-off. Waveforms at the boundary of the internal body diode.

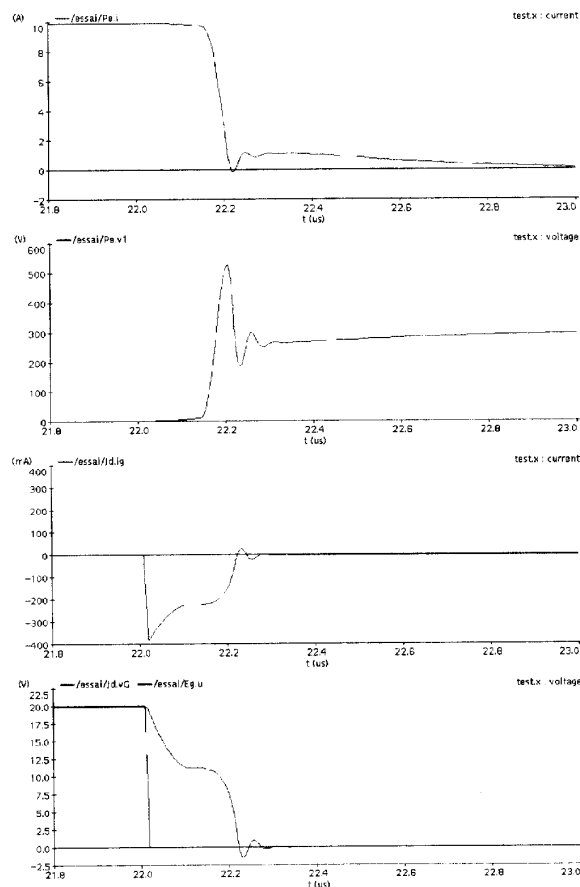


figure 17 : typical IGBT voltage and current waveforms during a turn-off.

We are working on the translation of our models to Saber with the language Mast. But the dynamic model switching and the change in the model causality are two problems to be overcome. These latter problems may be solved by adding implicit and artificial state-equations. Such tricks may be very expensive during simulation.

## VI - REFERENCES

- [1] O. Hamel, H. Morel, K. Besbes, J.P. Chante, "Behavioural simulation of diode devices in power systems", Proceedings of the 12th conference IMACS, Paris, France, 1998, Jul. 18-22, vol. 3, pp 219-223.
- [2] H. Morel, S.H. Gamal, J.P. Chante, "State-variable modelling of the Pin diode using an explicit approximation of the semiconductor device equations : a novel approach", to be soon published in IEEE Transactions on Power Electronics.
- [3] B. Allard, H. Morel, J.P. Chante, "State-variable modeling of the high-level injection regions in power devices. Application to power system simulation", Proceedings of the conference IEEE PESC'92, Toledo, Spain, 1992, June 29-July 3, vol. 2, pp 885-892.
- [4] B. Allard et al., "A novel simulation of the power BJT", Proceedings of the conference IEEE ISCAS, 1992, San Diego, Cal., vol. 2, pp 754-757.
- [5] B. Allard et al., "Reusing basic semiconductor region models in power device bond graph definition", Proceedings of the conference EPE'93, 1993, Brighton, UK, Sept. 13-16, pp 34-39.
- [6] D. Metzner, T. Volger, D. Schröder, "A modular concept for the circuit simulation of bipolar semiconductor devices", Proceedings of the conference EPE'93, 1993, Brighton, UK, Sept. 13-16.
- [7] P.O. Lauritzen, C.L. Ma, "A simple power diode model with reverse recovery", IEEE Transactions on Power Electronics, 1991, vol. 6, n. 2, pp 188-191.
- [8] P.O. Lauritzen et al., "A physically-based lumped-charge PnN diode model", Proceedings of the conference EPE'93, 1993, Brighton, UK, Sept. 13-16.
- [9] H. Morel, "Modélisation et simulation des composants et des systèmes de puissance", Professor Doctorate dissertation, INSA de Lyon, Lyon, France, 1994.
- [10] D. Karnopp and R. Rosenberg, "System dynamics : a unified approach", New-York, Wiley and Sons, 1975.
- [11] B. Allard, H. Morel, J.P. Chante, "Power electronic circuit simulation using bond graph and Petri network techniques", Proceedings of the conference IEEE PESC'93, Seattle, Wa., Jun. 21-25, 1993.
- [12] S. Selberherr, "Analysis and simulation of semiconductor device", Wien, Springer-Verlag, 1984.
- [13] C.C. Lin, B. Allard, H. Morel, "Technological parameter identification of the pindioe using transient signal parameter fit", Proceedings of the conference EPE'93, 1993, Brighton, UK, Sept. 13-16, pp 29-33.
- [14] "PACTE v0.9.1 : user's guide", Centre de Génie Electrique de Lyon, Lyon, France, 1994.
- [15] A.R. Hefner, "Analytical modelling of device-circuit interactions for the power insulated gate bipolar transistor (IGBT)", IEEE Transactions on Industry Applications, 1990, vol. 26, n° 6.